

# Microlensing and event rate of static spherically symmetric wormhole

Ke Gao<sup>1,\*</sup> and Lei-Hua Liu<sup>1,†</sup>

<sup>1</sup>*Department of Physics, College of Physics, Mechanical and Electrical Engineering, Jishou University, Jishou 416000, China*

Since the lensing effects play a vital role in modern cosmology. A new framework is developed for the static spherically symmetrical wormhole (WH) in terms of the radial equation of state (REoS). Following the standard procedure, we calculate the lensing equation, magnification, and event rate according to REoS, where our analysis indicates that the image problem of light source is complicated. As for the event rate, our investigations indicate that the larger values for the throat radius of WH and REoS will lead to larger values of the event rate. Compared with the event rate of blackhole, it is also claimed that the value of WH will be larger, in which their mass and the distance of them (blackhole or WH) between the light source and observer are comparable. Thus, our study could provide a possibility for distinguishing the WH and blackhole under similar circumstances.

## I. INTRODUCTION

The first research of WH originated from the inside of Schwarzschild's blackhole [1]. Thereafter, Einstein and Rosen explicitly proposed a vacuum solution that connects two remote regimes [2]. Ref. [3] firstly introduced the concept of WH. Then, the most simple WH named the Ellis WH was found by [4] whose ADM mass is zero. To traverse the WH, one kind of traversable WH was introduced by [5]. Then, the wormhole was extensively studied by [6–19]. The way for realizing the WH, the introduction of exotic matter is mandantory whose energy density is negative, which would violate the Null energy condition (NEC) [20–23].

After all the WH is just a hypothetic object predicted by General Relativity. To detect its existence, the lensing effects played a vital role in observations. Once again, Einstein also was the first one to develop the lensing equation, which proposed the well-known concept "Einstein angle" [24]. With the development of the technology for observation, gravitational lensing has become a standard method to detect astral objects including WH, dwarf, blackhole *e.t.c.* In modern astronomy, lensing mainly contains weak gravitational lensing, strong gravitational lens, and microlensing. Weak lensing was caused by the weak potential of the gravitational source which only slightly distorts the light as passing through some gravitational source [25, 26]. While for the strong lensing effects, the situation is the opposite, the potential of gravitational source, including WH, blackhole, and so on, is so strong that leads to the strong distortion of the light [27, 28]. The microlensing effect is an astronomical phenomenon caused by the weak gravitational lensing effect, which is used to detect objects from planetary mass to stellar mass. In this paper, we will focus on the microlensing effects. Refs. [29, 30] implemented the microlensing effect to explore WH. Thereafter, such extensive research of microlensing effects for WH were

investigated by [31–52]. Being similar with optics, the gravitational source will bend the light, thus one can observe several images of light source after bending the light. How many images can be formed after bending the light that naturally became a question in the lensing effects, which was discussed in [32, 37, 43, 47].

Distinguishing the WH and blackhole is always an essential goal, especially from observation. As an attempt, our previous work tried to utilize magnification for distinguishing them [31]. However, this method was so difficult since the distance of the target object between the light source and gravitational source is un-fixed, which leads to the magnification always changing. To provide more possibilities, we will implement the REoS to re-formulate the magnification under Gauss-Bonnet Theorem (GBT). The most significant quantity is the deflection angle. There were so many works related to the deflection angle in terms of GBT [53–64]. We will make use of REoS to investigate the event rate of WH, then it will be compared with blackhole when their mass and the distance between the light source and observer are comparable.

This paper is organized as follows: In Sec. II, the REoS will be implemented to rewrite the static spherically symmetrical metric. In Sec. III, we will use GBT to calculate the deflection angle and lensing equation in light of REoS, meanwhile, the magnification and event rate will be discussed, which are also explicitly related to REoS. In Sec. IV, we will give our conclusions and outlook.

## II. BASICS OF WH

In this section, we follow the notation in Refs. [65–67]. By starting with a spherically symmetrical metric,

$$ds^2 = -e^{2\Phi} dt^2 + \frac{dr^2}{1 - b(r)/r} + r^2 d\Omega^2, \quad (1)$$

which describes a generic static and spherically symmetrical WH metric. By assuming the application of a perfect fluid, its corresponding Einstein equation can be de-

\*Electronic address: 2021700389@stu.jsu.edu.cn

†Electronic address: liuleihua8899@hotmail.com

rived as follows,

$$p'_r = \frac{2}{r}(p_t - p_r) - (\rho + p_r)\Phi', \quad (2)$$

$$b' = 8\pi G\rho(r)r^2, \quad (3)$$

$$\Phi' = \frac{b + 8\pi Gp_r r^3}{2r^2(1 - b(r)/r)}, \quad (4)$$

where the prime denotes a derivative with respect to the radial coordinate  $r$ ,  $p_r$  represents the pressure in the radial component,  $p_t$  indicates the tangential pressure and  $\rho$  is the energy density. REoS is defined as follows,

$$p_r = \eta\rho. \quad (5)$$

where  $\eta$  represents REoS. The flaring-out condition and asymptotic flatness take the necessary condition:

$$\eta > 0 \text{ or } \eta < -1. \quad (6)$$

Moreover, it should be noticed that  $\eta > 0$  is possible only if  $\rho < 0$ . Combining Eqs. (2)-(5), one can get

$$b(r) = r_0 \left( \frac{r_0}{r} \right)^{\frac{1}{\eta}} e^{-(2/\eta)[\Phi(r) - \Phi(r_0)]} \times \left[ \frac{2}{\eta} \int_{r_0}^r \left( \frac{r}{r_0} \right)^{(1+\eta)/\eta} \Phi'(r) e^{(2/\eta)[\Phi(r) - \Phi(r_0)]} dr + 1 \right]. \quad (7)$$

Since we focus on the microlensing effects, it means that the potential of WH is quite weak. For simplicity, one can reasonably assume that  $\Phi(r) \approx \text{constant} = \Phi(r_0)$ . More precisely, the potential varies very slowly from the initial value  $\Phi(r_0)$ . Therefore, the impact parameter can be simplified into

$$b(r) = r_0 \left( \frac{r_0}{r} \right)^{\frac{1}{\eta}}. \quad (8)$$

Substitute this simplified impact parameter (8) into Eq. (1), then the metric can be transformed towards,

$$ds^2 = -Adt^2 + \frac{dr^2}{1 - (r_0/r)^{1+\frac{1}{\eta}}} + r^2 d\Omega^2, \quad (9)$$

where  $A = e^{2\Phi}$ . One can easily observe that metric (9) will become an Ellis-Bronnikov WH if the factor  $A$  was absorbed into temporal part and  $\eta = 1$ . Next section, we will implement REoS to investigate the microlensing effect of metric (9).

### III. MICROLENSING

In this section, we will calculate the magnification and the event rate of metric (9). First and foremost, the GBT will be implemented for further investigations.

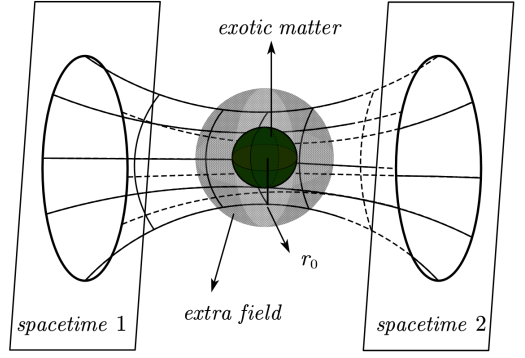


FIG. 1: A brief illustration of WH. The WH is connecting two remote regimes of spacetime. In our case, we consider the lensing effects occurring on one side of the WH that is in spacetime 1 or spacetime 2.

#### A. Deflection angle

In lensing effects including microlensing, the most essential quantity is the deflection angle, which will be calculated by GBT under the weak field approximation. Before introducing GBT, the optical Gaussian curvature will be computed, where the photon is traveling, thus the metric is the light-like case corresponding to  $ds^2 = 0$ . Our calculation can be performed in the equatorial plane due to the spherical symmetry. Then, the metric (9) will become

$$dt^2 = \frac{dr^2}{A \left( 1 - (r_0/r)^{1+\frac{1}{\eta}} \right)} + \frac{r^2}{A} d\phi^2. \quad (10)$$

For convenience, we introduce two auxiliary quantities:  $du = \frac{dr}{\sqrt{A(1 - (r_0/r)^{1+\frac{1}{\eta}})}}$  and  $\xi = \frac{r}{\sqrt{A}}$ . Gaussian optical curvature can be expressed as,

$$K = \frac{-1}{\xi(u)} \left[ \frac{dr}{du} \frac{d}{dr} \left( \frac{dr}{du} \right) \frac{d\xi}{dr} + \left( \frac{dr}{du} \right)^2 \frac{d^2 \xi}{dr^2} \right], \quad (11)$$

combine with metric (10), one can get

$$K = \frac{-\sqrt{A} r_0 \left( \frac{r_0}{r} \right)^{\frac{1}{\eta}} \left( 1 + \frac{1}{\eta} \right)}{2r^3 \sqrt{1 - \left( \frac{r_0}{r} \right)^{1+\frac{1}{\eta}}}}. \quad (12)$$

Once obtaining the Gaussian curvature, we could introduce the GBT whose formula is given by

$$\int \int_D K dS + \int_{\partial D} \kappa dt + \sum_i \alpha_i = 2\pi \chi(D), \quad (13)$$

where  $D$  is the integral domain denoted in Fig. 2. Choosing  $OS$  as the geodesic line, thus the integral along  $OS$  is zero. Besides, this Euler index  $\chi$  is one in domain  $D$ . Then, GBT (13) will become

$$\int \int_D K dS + \int_{\gamma_P} \kappa dt + \sum_i \alpha_i = 2\pi. \quad (14)$$

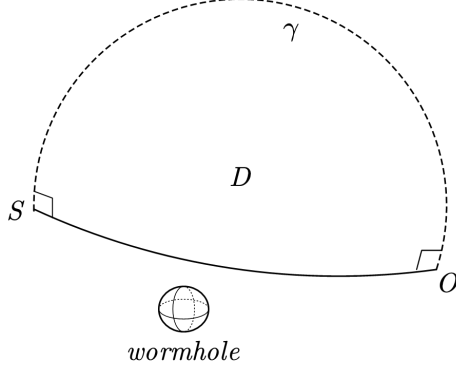


FIG. 2: Illustration of the GBT integral domain.  $O$  is the observer, and  $S$  is the light source. The region  $D$  represents the integral domain of the GBT, and integrating over this domain gives us the total deflection angle experienced by the light.

One can set  $\gamma$  to vertically intersect with geodesic line  $OS$  at point  $O$  and point  $S$ , Then the sum of external angles is  $\pi$  as showing

$$\sum_i \alpha_i = \frac{\pi}{2}(S) + \frac{\pi}{2}(O) = \pi. \quad (15)$$

Then, an integral transformation can be done as follows,

$$\kappa dt = \kappa \frac{dt}{d\phi} d\phi. \quad (16)$$

Here  $\phi$  is some kinds of angular coordinate where the gravitational source  $W$  is the central point as showing in Fig. 3. It can be done to set up  $\kappa \frac{dt}{d\phi} = 1$  on  $\gamma$ , therefore we have

$$\int \int_D K dS + \int_{\phi_O}^{\phi_S} d\phi + \pi = 2\pi. \quad (17)$$

Geodesic line  $OS$  could approximate to be a straight line. Due to the existence of lensing effects, the range of  $\phi$  could span from zero (at point  $O$ ) to  $\pi + \alpha$  (at point  $S$ ), where  $\alpha$  is the so-called deflection angle,

$$\int \int_D K dS + \int_0^{\pi+\alpha} d\phi + \pi = \int \int_D K dS + \pi + \alpha + \pi = 2\pi. \quad (18)$$

Then, the deflection angle is obtained as follows,

$$\alpha = - \int \int_D K dS. \quad (19)$$

Being armed with previous calculations for Gaussian curvature (12), the deflection angle can be furtherly determined by

$$\alpha = - \int_0^\pi \int_{\frac{b}{\sin \phi}}^\infty K \sqrt{\det h_{ab}} dr d\phi, \quad (20)$$

where  $b$  is impact parameter and  $h_{ab}$  is the optical metric in terms of  $u$  and  $\phi$ . Substituting Eq. (12) to (20), one can obtain

$$\alpha = \int_0^\pi \int_{\frac{b}{\sin \phi}}^\infty \frac{r_0 \left(\frac{r_0}{r}\right)^{\frac{1}{\eta}} \left(1 + \frac{1}{\eta}\right)}{2\sqrt{A} r^2 \left(1 - \left(\frac{r_0}{r}\right)^{1+\frac{1}{\eta}}\right)} dr d\phi. \quad (21)$$

Under the weak field approximation  $\frac{r_0}{r} \ll 1$ ,

$$\alpha = \frac{\sqrt{\pi} \left(\frac{r_0}{b}\right)^{1+\frac{1}{\eta}} \eta \Gamma[1 + \frac{1}{2\eta}]}{2\sqrt{A} \Gamma[\frac{1}{2}(3 + \frac{1}{\eta})]}, \quad \text{if } \frac{1}{\eta} > -2. \quad (22)$$

Being armed with deflection angle (22), one can investigate its corresponding lensing equation. As for the special case of  $A = 1$  and  $\eta = 1$ , our metric becomes the Ellis-Bronnikov WH:

$$ds^2 = -dt^2 + \frac{dr^2}{1 - \left(\frac{r_0}{r}\right)^2} + r^2 d\Omega^2. \quad (23)$$

The deflection angle for Eq. (21) ( $\eta = 1$ ) is given by

$$\alpha = \frac{\pi}{4} \left(\frac{r_0}{b}\right)^2, \quad (24)$$

where it is agreed with Refs. [31, 68, 69] in the first order.

## B. Lensing equation

According to Fig. 3, the plane geometry could yield the lensing equation

$$\beta = \theta - \frac{D_{LS}}{D_S} \alpha. \quad (25)$$

Substitute Eq. (22) to Eq. (25), one can obtain that

$$\theta^{2+\frac{1}{\eta}} - \beta \theta^{1+\frac{1}{\eta}} - \frac{D_{LS}}{D_S} \frac{\sqrt{\pi} \left(\frac{r_0}{D_L}\right)^{1+\frac{1}{\eta}} \eta \Gamma[1 + \frac{1}{2\eta}]}{2\sqrt{A} \Gamma[\frac{1}{3}(3 + \frac{1}{\eta})]} = 0, \quad (26)$$

where we have used the approximation  $b \approx \theta D_L$ . According to Eq. (26), one can explicitly obtain the relation between the order of lensing equation ( $n$ ) and  $\eta$ ,

$$n = 2 + \frac{1}{\eta}. \quad (27)$$

This is an equation about the number of images for light source (If there are  $n$  various real solutions of the  $n - th$  order equation). When  $\eta \rightarrow 0_+$ , then  $n \rightarrow \infty$ , this means that we can at most get an infinite numbers of image. On the other hand, when  $\eta \rightarrow \pm\infty$ , it expects to be two images as showing in Einstein ring. However, the realistic situation is more complicated. One can actually obtain  $n$  solutions of lensing Eq. (26), in which some of them are complex solutions that one cannot observe its corresponding images. We take  $\eta = 1$  as an illustration since

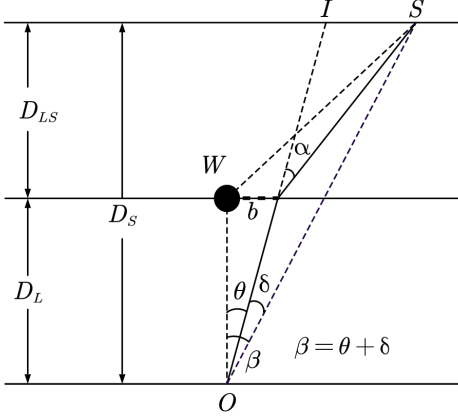


FIG. 3: Showing lens plane geometry.  $I$  is the location of image of light source,  $S$  is location of light source,  $\alpha$  is the deflection angle,  $W$  is the WH and  $b$  is the impact parameter. All of these angles are much less than unity.

the charged WH [70] and WH with quantum corrections [71], *e.t.c.*, are all in this case. Thereafter, lensing equation (26) becomes

$$\theta^3 - \beta\theta^2 - M = 0, \quad (28)$$

where we have set  $\frac{D_{LS}}{D_S} = \frac{1}{2}$  for simplicity and  $M = \frac{\pi}{16\sqrt{A}\Gamma[4/3]} \frac{r_0^2}{D_L^2} > 0$ . Lensing equation (28) is the third order equation in terms of  $\theta$ , in which its overall discriminant  $\Delta > 0$  in light of appendix I in [32]. Thus, there is only a real solution for Eq. (28) corresponding to only one image of the light source. As for the second order of

$\theta$ , the value of  $\eta$  is huge whose value will set to be 10, then the lensing equation (26) will be written by

$$\theta^2 - \beta\theta - \frac{5}{2\sqrt{A}} \frac{r_0}{D_L} = 0, \quad (29)$$

where we also have set  $\frac{D_{LS}}{D_S} = \frac{1}{2}$  and its overall discriminant is also larger than zero, thus it will be of two real solutions corresponding to two images of the light source. When  $n = 4$  and  $\sqrt{\frac{\pi}{A}} \frac{1}{8\Gamma[5/3]} \frac{r_0^3}{D_L^3} = 0.08$ , the lensing equation (26) could have four real solutions corresponding to the four images of light source. As for the higher order equation of  $\theta$  ( $n > 4$ ), it is more complicated whose real solutions are difficult to determine. Although we have obtained the explicit relation  $n = 2 + 1/\eta$ , the number of images of the light source is still not figured out in some sense.

### C. Magnification

Similar to optics, the images of the light source will be magnified or demagnified due to varying the cross-section of light rays, whose definition is determined by the ratio between distinct solid angles,

$$\mu_{\text{total}} = \sum_i \left| \frac{\beta}{\theta_i} \frac{d\beta}{d\theta_i} \right|^{-1}, \quad (30)$$

where  $\theta_i$  is the angle of the  $i$ -th image of light source. Substituting Eq. (25) into Eq. (30), which leads to

$$\mu = \left| \frac{\pi D_L D_{LS} 2^{-\frac{1}{\eta}-2} r_0 \left(\frac{r_0}{b}\right)^{1/\eta} \left( \sqrt{A} b^2 D_S \Gamma\left(2 + \frac{1}{\eta}\right) - D_L D_{LS} 2^{1/\eta} \eta (\eta + 1) r_0 \Gamma\left(1 + \frac{1}{2\eta}\right)^2 \left(\frac{r_0}{b}\right)^{1/\eta} \right)}{A b^4 D_S^2 \Gamma\left(\frac{1}{2}\left(3 + \frac{1}{\eta}\right)\right)^2} + 1 \right|^{-1}. \quad (31)$$

Eq. (31) provides a general formula for calculating the magnification of the static spherically symmetric WH. Due to the flaring-out condition (6), REoS can be divided into two regimes:  $(-\infty, -1)$  and  $(0, \infty)$ . We have chosen specific values of  $\eta$  to investigate the magnification including in Figs. 4 and 5.

The trend of magnification in Figs. 4 and 5 are the same, which there is only one peak. With the enhancement of the value of  $\eta$ , the position of the corresponding magnification peak will occur in larger values of  $b$ . Thus, the cases of  $\eta = 2, 5, -1$  are not shown in Figs. 4 and 5, in which one cannot observe any image of light source since the magnification is zero in this scale (the range

of  $b$  as showing in Figs. 4 and 5). The total varying trend is that: the demagnification will appear at some certain scale, thereafter the magnification will approach the maximal value (the peak of magnification), and finally it will tend to be one that the size of image of light source is the same with the light source itself. The value of  $\eta$  could highly impact the position of the peak of magnification since it mainly influences the mass of WH whose details will be thoroughly investigated in Sec. IIID. A simple analysis could understand this physical picture, the larger mass of WH will more significantly distort the image of light source.

For completeness, we also give a plot of magnification

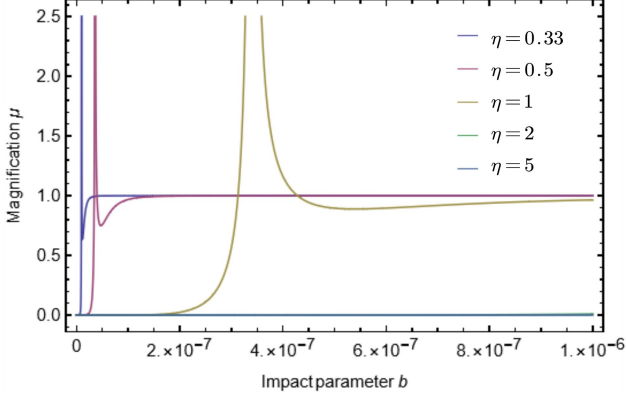


FIG. 4: In the case of  $\eta > 0$ , the magnification given by Eq. (31) varies with the impact parameters  $b$  (Unit: kpc), and the legend in the figure indicates the corresponding REoS values for different curves. Here we set the parameters as follows:  $D_S = 2D_L = 2D_{LS} = 20$  kpc,  $r_0 = 1 \times 10^{-10}$  kpc, and  $A = 1$ . According to  $n = 2 + \frac{1}{\eta}$ ,  $n = 5$  with  $\eta = \frac{1}{3}$ ,  $n = 4$  with  $\eta = \frac{1}{2}$  and  $n = 3$  with  $\eta = 1$ , in which the peak is not including  $\eta = 2, 5$  since it is beyond the scope.

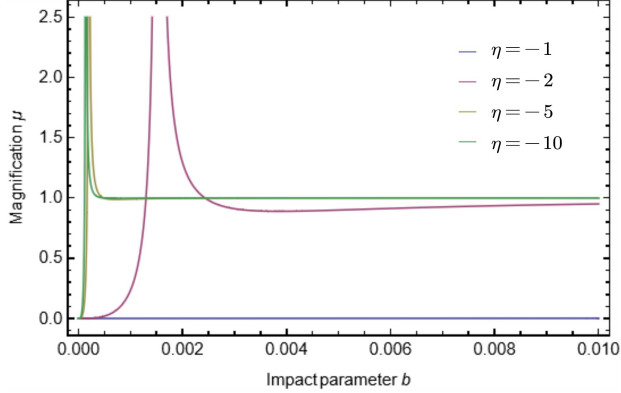


FIG. 5: In the case of  $\eta < -1$ , the magnification given by Eq. (31) also varies with the impact parameters  $b$ , and the legend in the figure indicates the corresponding REoS values for different curves. We set the parameters as follows:  $D_S = 2D_L = 2D_{LS} = 20$  kpc,  $r_0 = 1 \times 10^{-10}$  kpc, and  $A = 1$ . The curves where  $\eta = -5$  and  $\eta = -10$  have almost overlapped. The case of  $\eta = -1$  corresponds to  $n = 1$  (only one image of light source) whose peak is also not included in this scale.

highly related to the radius  $r_0$  of WH as shown in Fig. 6. The total trend is also the same only containing one peak of magnification. With the larger values of  $r_0$ , the position of the peak will appear in larger values of  $b$  since the  $r_0$  explicitly relates to the mass of WH. We need to emphasize that the demagnification of Kerr blackhole will be influenced by its angular momentum [72, 73], thus we may extend our method to the rotating blackhole and WH. To sum up, the factor who influences the mass of WH will highly impact the position of the peak of  $\mu$ .

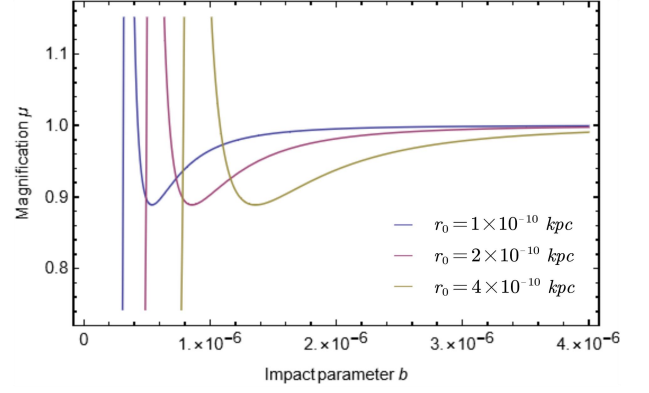


FIG. 6: The magnification varies with the radius  $r_0$  of throat for WH. The various values of  $r_0$  correspond to different curves indicated in the legend. We set the parameters as follows:  $D_S = 2D_L = 2D_{LS} = 20$  kpc,  $\eta = 1$ ,  $A = 1$ .

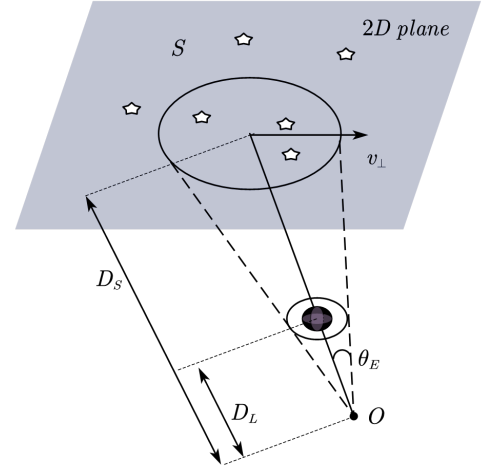


FIG. 7: The illustration of the microlensing rate of WH moving along this 2D plane. This 2D plane is the source plane, and we assume that the number of sources within the Einstein ring is  $\chi\sigma_{micro}$ .

#### D. Event rate

The microlensing effect is a rare phenomenon in observations. To describe the probability of this event, we need to calculate the optical depth  $\tau$ . The optical depth represents the probability of observing the microlensing event of a source at a certain location  $D_S$ , which reflects the number of microlensing events per unit of time. If we observe  $N$  light sources, we can calculate the microlensing event rate  $\Gamma = \frac{d(N\tau)}{dt}$ . Here, we aim to develop an analytic formula for calculating the event rate under the metric (9). For better understanding the event rate, we give a Fig. 7 as an illustration.

Our work is begun by metric (9). First, the effective

mass of WH comes via Ref. [74] that is defined by

$$M = \frac{r_0}{2} + \int_{r_0}^r 4\pi\rho(r')r'^2 dr', \quad (32)$$

where the energy density can be found in light of Einstein equation,

$$\rho = -\frac{Ar_0\left(\frac{r_0}{r}\right)^{\frac{1}{\eta}} c^4}{r^3\eta} \frac{1}{8\pi G}. \quad (33)$$

Therefore, the effective mass can be derived by

$$M = \frac{Ac^4 r_0 \left(\frac{r_0}{D_L}\right)^{\frac{1}{\eta}}}{2G} - \frac{Ac^4 r_0}{2G} + \frac{r_0}{2}, \quad (34)$$

where the integration range is from  $r_0$  to  $D_L$  as showing in Fig. 7. Before calculating the event rate, what we need is the Einstein angle whose definition is  $\theta_E = \frac{D_{LS}}{D_S}\alpha$  in light of (25). Then we could implement Eq. (22) to plug into the definition of Einstein angle, one can obtain

$$\theta_E = \left(\frac{r_0}{D_L}\right)^{\frac{1+\frac{1}{\eta}}{2+\frac{1}{\eta}}} \left(\frac{\sqrt{\pi}\eta\Gamma[1+\frac{1}{2\eta}]}{2\sqrt{A}\Gamma[\frac{1}{2}(3+\frac{1}{\eta})]} \frac{D_{LS}}{D_S}\right)^{\frac{1}{2+\frac{1}{\eta}}}, \quad (35)$$

where it is explicitly related to Einstein ring where light source, gravitational lensing source and observer are aligned. Once obtaining the Einstein angle, one could also define the cross-section for microlensing as follows,

$$\sigma_{micro} = \pi\theta_E^2, \quad (36)$$

where it is the solid angle producing a detectable microlensing signal. Due to the relative motion between the light source and lens, one can also define the Einstein radius crossing time

$$t_E = \frac{r_E}{v} = \frac{D_S\theta_E}{v}, \quad (37)$$

where  $v$  is the relative velocity between the light source and lensing source as shown in Fig. 7. For simplification, the lensing source could be fixed and the light source is travelling at speed  $v$  whose direction is also showing in Fig. 7. The optical depth gives rise to a detectable probability of microlensing event, which defines as follows,

$$\tau = \frac{1}{\Omega} \int_0^{D_S} \sigma_{micro} dN_L, \quad (38)$$

In a simple analysis, the number of lens sources is changing as varying with  $D_L$ . Therefore, we could further derive that

$$dN_L = \Omega D_L^2 n(D_L) dD_L. \quad (39)$$

Then, the optical depth is

$$\tau(D_S) = \frac{1}{\Omega} \int_0^{D_S} [\Omega D_L^2 n(D_L)] (\pi\theta_E^2) dD_L. \quad (40)$$

There is only one lensing source, its energy density is a constant which leads to  $n(D_L) = \frac{\rho}{m}$ . Therefore, we have

$$\tau(D_S) = \int_0^{D_S} D_L^2 \frac{\rho(D_L)}{M} \pi\theta_E^2 dD_L. \quad (41)$$

The integration interval is  $(0, D_S)$ , which can be divided into  $(D_L, r_0) \cup (r_0, D_{LS})$  according to Fig. 3. In the interval  $(0, r_0)$ , the integration of (41) is zero since we have neglected the inner structure of WH. Then, we set parameters as  $c = G = A = 1$  and  $D_S = 2D_L = 2D_{LS}$ . Finally, our integration result is

$$\left| \frac{\left(\frac{\sqrt{\pi}\eta\Gamma[1+\frac{1}{2\eta}]}{2\Gamma[\frac{1}{2}(3+\frac{1}{\eta})]} \frac{D_{LS}}{D_S}\right)^{\frac{2}{2+\frac{1}{\eta}}} \left(r_0^{\frac{2(1+\eta)}{1+2\eta}} D_{LS}^{-\frac{2(1+\eta)}{1+2\eta}} - 1\right) (1+2\eta)}{4\eta(1+\eta)} \right|. \quad (42)$$

The absolute value comes via the positivity of probability. We can differentiate the optical depth in light of Eq. (3),

$$d\tau = \frac{1}{\Omega} \int_0^{D_S} n(D_L) \Omega 2r_E v dt dD_L = \int_0^{D_S} 2n(D_L) r_E^2 \frac{dt}{t_E} dD_L. \quad (43)$$

We may observe the microlensing event, while we are monitoring a certain number of light sources  $N$  (dubbed as constant) within a specific time, its corresponding event rate is defined as

$$\Gamma = \frac{d(N\tau)}{dt} = \frac{2N}{\pi} \int_0^{D_S} n(D_L) \frac{\pi r_E^2}{t_E} dD_L = \frac{2N}{\pi t_E} \tau. \quad (44)$$

Substituting the previous calculation results Eq. (37) and Eq. (42) into Eq. (44), we obtain

$$\Gamma = \frac{2\chi\sigma_{micro}}{\pi \frac{D_S}{v} \left(\frac{r_0}{D_L}\right)^{\frac{1+\frac{1}{\eta}}{2+\frac{1}{\eta}}} \left(\frac{\sqrt{\pi}\eta\Gamma[1+\frac{1}{2\eta}]}{2\Gamma[\frac{1}{2}(3+\frac{1}{\eta})]} \frac{D_{LS}}{D_S}\right)^{\frac{1}{2+\frac{1}{\eta}}}} \times \left| \left(\frac{\sqrt{\pi}\eta\Gamma[1+\frac{1}{2\eta}]}{2\Gamma[\frac{1}{2}(3+\frac{1}{\eta})]} \frac{D_{LS}}{D_S}\right)^{\frac{2}{2+\frac{1}{\eta}}} \frac{\left(r_0^{\frac{2(1+\eta)}{1+2\eta}} D_{LS}^{-\frac{2(1+\eta)}{1+2\eta}} - 1\right) (1+2\eta)}{4\eta(1+\eta)} \right|. \quad (45)$$

$\eta$	$\chi$	$v$ m/s	$r_0$ m	$Mass$ $M_\odot$	$\theta_E$ rad	$r_E$ m	$t_E$ year	$\tau$	$\Gamma$ year $^{-1}$
-10	$1.00 \times 10^{14}$	$3.00 \times 10^4$	$3.24 \times 10^9$	$1.38 \times 10^7$	$\mathbb{C}$	$\mathbb{C}$	$\mathbb{C}$	0.297	$\mathbb{C}$
-2	$1.00 \times 10^{14}$	$3.00 \times 10^4$	$3.24 \times 10^9$	$3.46 \times 10^{11}$	$\mathbb{C}$	$\mathbb{C}$	$\mathbb{C}$	0.477	$\mathbb{C}$
-1.1	$1.00 \times 10^{14}$	$3.00 \times 10^4$	$3.24 \times 10^9$	$1.09 \times 10^{16}$	$\mathbb{C}$	$\mathbb{C}$	$\mathbb{C}$	1.84	$\mathbb{C}$
0.33	$1.00 \times 10^{14}$	$3.00 \times 10^4$	$3.24 \times 10^9$	$\approx 0$	$9.67 \times 10^{-10}$	$6.25 \times 10^{11}$	0.660	0.374	$1.06 \times 10^{-4}$
0.5	$1.00 \times 10^{14}$	$3.00 \times 10^4$	$3.24 \times 10^9$	$\approx 0$	$3.59 \times 10^{-9}$	$2.32 \times 10^{12}$	2.46	0.272	$2.86 \times 10^{-4}$
1	$1.00 \times 10^{14}$	$3.00 \times 10^4$	$3.24 \times 10^9$	$1.09 \times 10^{-5}$	$3.40 \times 10^{-8}$	$2.20 \times 10^{13}$	23.2	0.201	$2.00 \times 10^{-3}$
1.5	$1.00 \times 10^{14}$	$3.00 \times 10^4$	$3.24 \times 10^9$	$5.08 \times 10^{-2}$	$1.12 \times 10^{-7}$	$7.25 \times 10^{13}$	76.7	0.189	$6.20 \times 10^{-3}$
2	$1.00 \times 10^{14}$	$3.00 \times 10^4$	$3.24 \times 10^8$	0.109	$5.98 \times 10^{-8}$	$3.87 \times 10^{13}$	40.9	0.187	$3.27 \times 10^{-3}$
2	$1.00 \times 10^{14}$	$3.00 \times 10^4$	$3.24 \times 10^9$	3.46	$2.38 \times 10^{-7}$	$1.54 \times 10^{14}$	163	0.187	$1.30 \times 10^{-2}$
2	$1.00 \times 10^{14}$	$3.00 \times 10^4$	$3.24 \times 10^{10}$	109	$9.48 \times 10^{-7}$	$6.13 \times 10^{14}$	648	0.187	$5.19 \times 10^{-2}$
2.5	$1.00 \times 10^{14}$	$3.00 \times 10^4$	$3.24 \times 10^9$	43.6	$4.02 \times 10^{-7}$	$2.60 \times 10^{14}$	274	0.188	$2.21 \times 10^{-2}$
3	$1.00 \times 10^{14}$	$3.00 \times 10^4$	$3.24 \times 10^9$	236	$5.92 \times 10^{-7}$	$3.83 \times 10^{14}$	405	0.191	$3.30 \times 10^{-2}$

TABLE I: The change of event rate  $\Gamma$  with  $\eta$ .  $\chi$  is the number of sources observed per unit angular area  $\pi\theta^2$ ,  $v$  is the relative velocity between the WH and the source plane,  $r_0$  is the throat radius of the WH. In terms of mass, we choose solar mass  $M_\odot$  as the unit,  $\theta_E$  is the Einstein angle,  $r_E$  is the Einstein radius, and  $\tau$  is the optical depth. We set the parameters  $D_S = 21$  kpc, and  $A = 1$ .

$r_0$ (km)	$3.24 \times 10^1$	$3.24 \times 10^2$	$3.24 \times 10^3$	$3.24 \times 10^4$	$3.24 \times 10^5$	$3.24 \times 10^6$	$3.24 \times 10^7$
$\Gamma$ (year $^{-1}$ )	$1.86 \times 10^{-6}$	$8.62 \times 10^{-6}$	$4.00 \times 10^{-5}$	$1.86 \times 10^{-4}$	$8.62 \times 10^{-4}$	$4.00 \times 10^{-3}$	$1.86 \times 10^{-2}$

TABLE II: The numerical results by Eq (45) : event rate  $\Gamma$  of Ellis-Bronnikov WH corresponding to throat radius  $r_0$ .  $D_S = 21$  kpc is assumed.  $v = 0.0001c$ ,  $\chi = 2 \times 10^{14}$  and  $n(D_L) = \frac{\rho}{M}$  are assumed.

$r_0$ (km)	10	$10^2$	$10^3$	$10^4$	$10^5$	$10^6$	$10^7$
$\Gamma$ (year $^{-1}$ )	$1.88 \times 10^{-14}$	$8.73 \times 10^{-14}$	$4.05 \times 10^{-13}$	$1.88 \times 10^{-12}$	$8.73 \times 10^{-12}$	$4.05 \times 10^{-11}$	$1.88 \times 10^{-10}$

TABLE III: The numerical results by [47]: The various event rates  $\Gamma$  of Ellis-Bronnikov WH correspond to different throat radius  $r_0$ .  $D_S = 8$  kpc is assumed.  $v = 5000$  km/s and  $n = 4.97 \times 10^{-9}$  pc $^{-3}$  are assumed.

where we express  $N$  as  $\chi\sigma_{micro}$ ,  $\chi \propto D_S^2$  is constant determined by observation.  $\chi$  has a significant impact on the event rate that leads to  $\Gamma \propto \chi$ . Comparing with [75–77], we reasonably set  $\chi = 1 \times 10^{14}$ ,  $D_S = 2D_L = 2D_{LS} = 21$  kpc and  $v = 3 \times 10^4$  m/s. Being armed with these parameters, one can determine the mass of WH and Einstein's angle. To illustrate how  $\eta$  impacts the event rate, all of our calculations are listed in Tab I. It indicates that the event rate and Einstein angle will be enhanced by increasing the value of  $\eta$  but not for optical depth. One could see that  $\Gamma$  is of order  $10^{-2}$  when there are two images per light source. Another point needs to be noticed is that it is meaningless as  $\eta < -1$  since the  $\Gamma$  is a complex number. Finally, it could be seen that there are at least two images per light source based on  $n = 2 + \frac{1}{\eta}$ . For completeness, we also give a plot to show how the radius  $r_0$  of WH impacts  $\Gamma$  shown in Fig. 8. It explicitly indicates that the event rate will be enhanced by increasing the value of  $r_0$ . We also show the results of [47] in Tab. III, where they computed the event rate of clusters in Ellis-Bronnikov WHs with different throat radii. It indicates that the event rate will be enhanced

by improving the value of throat radii which supports our numerical results. Their results are different from ours since they consider the cluster of WHs. It leads to the mass becoming sparse which is different from our assumption, where we only consider one WH as the lens source whose energy density is larger. To sum up, the event rate will be larger as increasing the value of  $\eta$  and  $r_0$ .

Additionally, we are curious if event rate can be used to distinguish between black holes and WHs. In Ref. [78], they implement the CMC Cluster Catalog model to study  $n8 - rv0.5 - rg8 - z0.1$  case, where the mass of lens is  $M = 2 \times 10^5 M_\odot$  and  $t = 12$  Gyr, then one can obtain the event rate  $< 10^{-5}$  year $^{-1}$  for the single black-hole. In comparison, we set  $\eta = 1$  and  $r_0 = 3.24 \times 10^{14}$  m corresponding to  $M = 1.1 \times 10^5 M_\odot$ . We could observe  $5.0 \times 10^5$  light sources with an Einstein radius crossing time of  $5.0 \times 10^5$  year. When the  $M$  and  $t$  converted into the  $n8 - rv0.5 - rg8 - z0.1$  case, its corresponding event rate is about  $10^{-2} \sim 10^{-3}$  year $^{-1}$ . Our estimation shows that the event rate of WH is two orders higher compared with blackhole as the mass and Einstein crossing time

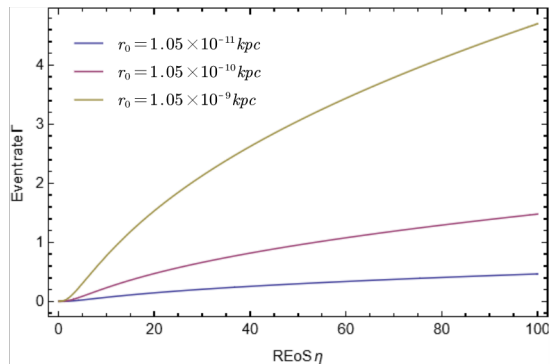


FIG. 8: The relationship between the number of microlensing events observed each year and REoS. Each curve in the figure corresponds to a different wormhole throat radius. We set other parameters consistent with Tab I.

are comparable. We should emphasize the importance of Tab. I, in which the observation can explicitly compare with our numerical results as fixing  $t$ , mass of WH, and the number of light sources. If it is compatible with our predictions, it could imply that the lensing object is WH and the value is smaller than ours which could be blackhole.

#### IV. CONCLUSION AND OUTLOOK

This paper presents a comprehensive investigation of the microlensing effects of the static spherically symmetric WH described by Eq. (9). By introducing the so-called REoS parameter  $\eta = \frac{p_r}{\rho}$ , we reformulate the metric, allowing us to re-examine the microlensing effect metric (9), including its magnification and event rate. We employ the GBT to calculate the deflection angle of metric (9) under the weak field approximation. The resulting lensing equation contains an explicit formula  $n = 2 + \frac{1}{\eta}$  that reflects the order of the lensing equation on the equatorial plane. We take  $\eta = 1$  ( $n = 3$ ) as an illustration, in which we have shown that there is only one real solution of lensing equation (26) since the overall discriminant is larger than zero, which means that there is only one image of the light source. As for  $n = 2$  (we have set  $\eta = 10$ ), it shows that there are two real solutions of (26). Even one could observe four images of the light source as  $n = 4$ , where we have fixed the values of  $\frac{r_0}{D_L}$ ,  $A$  and  $D_{LS}/D_S$ . For a higher-order lensing equation, it is more complicated. In some sense, the image problem of the light source is still not worked out due to

the complication of lensing equation (26).

In order to reformulate the lensing equation, we also derive a general formula for calculating the magnification in terms of REoS. This formula allows us to analyze how the magnification changes with REoS and the WH throat radius  $r_0$ . Our analysis reveals that the larger values of  $\eta$  will lead to the position of magnification's peak located at the larger values of impact parameter  $b$  as shown in Figs. 4 and 5. A similar trend is applied for the radius of the throat of WH as shown in Fig. 6. To provide a more complete analysis, we also perform the analytical calculations of event rate for a single WH source. We mainly list our numerical results in Tab. I and Fig. 8, which clearly indicates that the larger values of  $\eta$  and  $r_0$  will cause the larger values of event rate. As one example of our metric, the investigation of Ref. [47] listed in Tab. III holds the same results as ours. Especially, our results as shown in Tab. I could provide an explicit comparison with observations as fixing  $t$ , mass of WH, and the number of light source, which guides for distinguishing the WH and blackhole via event rate.

Our work is just a preliminary investigation of a single gravitational source. The lensing effects can be applied to more realistic situations, *i.e.* the primordial blackhole plays an important role of dark matter, we could extend our method to this direction [79]. Another natural extension is for the microlensing of the clusters of galaxy [78]. One can utilize the approximated metric to mimic their dynamical background. The difference comes via the energy-momentum tensor. Further, we could also extend our method to the strong lensing regime that may include the topological effects of spacetime, in which the deflection angle and lensing equation are different. To fully address this issue, the calculation technology should be developed.

#### Acknowledgements

We appreciate that Hai-Qing Zhang and Bi-Chu Li give lots of suggestions to improve this manuscript. And we are also grateful to Prof. Wentao Luo that he gives professional guidance on some concepts of microlensing. We are very grateful for the critical reading from Dr. Xin-Fei Li. LH and KG are funded by NSFC grant NO. 12165009 and Hunan Natural Science Foundation NO. 2023JJ30487.

#### References

- 
- [1] Ludwig, Flamm, Beitrage zur Einstein schen gravitations theorie. Hirzel, 1916.
  - [2] Albert Einstein and Nathan Rosen. "The particle problem in the general theory of relativity". In: Physical Review 48.1 (1935), p. 73.
  - [3] Charles W Misner and John A Wheeler. physics 2.6



- (1957), pp. 525–603.
- [4] Homer G Ellis, *Journal of Mathematical Physics* **14**.1 (1973), pp. 104–118.
- [5] M. S. Morris and K. S. Thorne, *Am. J. Phys.* **56** (1988), 395–412 doi:10.1119/1.15620
- [6] T. Damour and S. N. Solodukhin, *Phys. Rev. D* **76** (2007), 024016 doi:10.1103/PhysRevD.76.024016 [arXiv:0704.2667 [gr-qc]].
- [7] W. T. Kim, J. J. Oh and M. S. Yoon, *Phys. Rev. D* **70** (2004), 044006 doi:10.1103/PhysRevD.70.044006 [arXiv:gr-qc/0307034 [gr-qc]].
- [8] P. Bueno, P. A. Cano, F. Goelen, T. Hertog and B. Vercnocke, *Phys. Rev. D* **97** (2018) no.2, 024040 doi:10.1103/PhysRevD.97.024040 [arXiv:1711.00391 [gr-qc]].
- [9] M. Visser, *Phys. Rev. D* **39** (1989), 3182–3184 doi:10.1103/PhysRevD.39.3182 [arXiv:0809.0907 [gr-qc]].
- [10] S. V. Sushkov, *Phys. Rev. D* **71** (2005), 043520 doi:10.1103/PhysRevD.71.043520 [arXiv:gr-qc/0502084 [gr-qc]].
- [11] K. A. Bronnikov and S. W. Kim, *Phys. Rev. D* **67** (2003), 064027 doi:10.1103/PhysRevD.67.064027 [arXiv:gr-qc/0212112 [gr-qc]].
- [12] G. Clement, *Phys. Rev. D* **51** (1995), 6803–6809 doi:10.1103/PhysRevD.51.6803 [arXiv:gr-qc/9502033 [gr-qc]].
- [13] M. G. Richarte, I. G. Salako, J. P. Morais Graça, H. Moradpour and A. Övgün, *Phys. Rev. D* **96** (2017) no.8, 084022 doi:10.1103/PhysRevD.96.084022 [arXiv:1710.05886 [gr-qc]].
- [14] I. Ayuso, F. S. N. Lobo and J. P. Mimoso, *Phys. Rev. D* **103** (2021) no.4, 044018 doi:10.1103/PhysRevD.103.044018 [arXiv:2012.00047 [gr-qc]].
- [15] M. Kord Zangeneh and F. S. N. Lobo, *Eur. Phys. J. C* **81** (2021) no.4, 285 doi:10.1140/epjc/s10052-021-09059-y [arXiv:2011.01745 [gr-qc]].
- [16] S. Q. Song and E. Güdekli, *New Astron.* **100** (2023), 101993 doi:10.1016/j.newast.2022.101993
- [17] R. Saleem, M. I. Aslam and K. Rasool, *Chin. J. Phys.* **82** (2023), 1–14 doi:10.1016/j.cjph.2022.12.015
- [18] A. Eid and A. Alkaoud, *New Astron.* **101** (2023), 102021 doi:10.1016/j.newast.2023.102021
- [19] N. Godani, *New Astron.* **100** (2023), 101994 doi:10.1016/j.newast.2022.101994
- [20] D. Hochberg and M. Visser, *Phys. Rev. Lett.* **81** (1998), 746–749 doi:10.1103/PhysRevLett.81.746 [arXiv:gr-qc/9802048 [gr-qc]].
- [21] D. Hochberg and M. Visser, *Phys. Rev. D* **58** (1998), 044021 doi:10.1103/PhysRevD.58.044021 [arXiv:gr-qc/9802046 [gr-qc]].
- [22] F. Lobo and P. Crawford, *Lect. Notes Phys.* **617** (2003), 277–291 doi:10.1007/3-540-36973-2\_15 [arXiv:gr-qc/0204038 [gr-qc]].
- [23] F. S. N. Lobo, *Gen. Rel. Grav.* **37** (2005), 2023–2038 doi:10.1007/s10714-005-0177-x [arXiv:gr-qc/0410087 [gr-qc]].
- [24] A. Einstein, *Science* **84** (1936), 506–507 doi:10.1126/science.84.2188.506
- [25] M. Bartelmann and P. Schneider, *Phys. Rept.* **340** (2001), 291–472 doi:10.1016/S0370-1573(00)00082-X [arXiv:astro-ph/9912508 [astro-ph]].
- [26] N. Kaiser, *Astrophys. J.* **388** (1992), 272 doi:10.1086/171151
- [27] V. Bozza, *Phys. Rev. D* **66** (2002), 103001 doi:10.1103/PhysRevD.66.103001 [arXiv:gr-qc/0208075 [gr-qc]].
- [28] K. S. Virbhadra and G. F. R. Ellis, *Phys. Rev. D* **62** (2000), 084003 doi:10.1103/PhysRevD.62.084003 [arXiv:astro-ph/9904193 [astro-ph]].
- [29] V. Perlick, *Living Rev. Rel.* **7** (2004), 9
- [30] C. Stoughton *et al.* [SDSS], *Astron. J.* **123** (2002), 485–548 doi:10.1086/324741
- [31] K. Gao, L. H. Liu and M. Zhu, [arXiv:2211.17065 [gr-qc]].
- [32] L. H. Liu, M. Zhu, W. Luo, Y. F. Cai and Y. Wang, *Phys. Rev. D* **107** (2023) no.2, 024022 doi:10.1103/PhysRevD.107.024022 [arXiv:2207.05406 [gr-qc]].
- [33] O. Sokoliuk, S. Prahara, A. Baransky and P. K. Sahoo, *Astron. Astrophys.* **665** (2022), A139 doi:10.1051/0004-6361/202244358 [arXiv:2207.07193 [gr-qc]].
- [34] K. Zatrimeylov, [arXiv:2108.13350 [astro-ph.CO]].
- [35] X. T. Cheng and Y. Xie, *Phys. Rev. D* **103** (2021) no.6, 064040 doi:10.1103/PhysRevD.103.064040
- [36] Z. Li and J. Jia, *Eur. Phys. J. C* **80** (2020) no.2, 157 doi:10.1140/epjc/s10052-020-7665-8 [arXiv:1912.05194 [gr-qc]].
- [37] M. Kuniyasu, K. Nanri, N. Sakai, T. Ohgami, R. Fukushige and S. Komura, *Phys. Rev. D* **97** (2018) no.10, 104063 doi:10.1103/PhysRevD.97.104063 [arXiv:1806.00231 [gr-qc]].
- [38] M. Raidal, S. Solodukhin, V. Vaskonen and H. Veermäe, *Phys. Rev. D* **97** (2018) no.12, 123520 doi:10.1103/PhysRevD.97.123520 [arXiv:1802.07728 [astro-ph.CO]].
- [39] N. Tsukamoto and Y. Gong, *Phys. Rev. D* **97** (2018) no.8, 084051 doi:10.1103/PhysRevD.97.084051 [arXiv:1711.04560 [gr-qc]].
- [40] S. N. Sajadi and N. Riazi, *Can. J. Phys.* **98** (2020) no.11, 1046–1054 doi:10.1139/cjpp-2019-0524 [arXiv:1611.04343 [gr-qc]].
- [41] R. Lukmanova, A. Kulbakova, R. Izmailov and A. A. Potapov, *Int. J. Theor. Phys.* **55** (2016) no.11, 4723–4730 doi:10.1007/s10773-016-3095-7
- [42] N. Tsukamoto and T. Harada, *Phys. Rev. D* **95** (2017) no.2, 024030 doi:10.1103/PhysRevD.95.024030 [arXiv:1607.01120 [gr-qc]].
- [43] T. Kitamura, *Gravitational lensing in an exotic space-time*
- [44] T. Kitamura, K. Nakajima and H. Asada, *Phys. Rev. D* **87** (2013) no.2, 027501 doi:10.1103/PhysRevD.87.027501 [arXiv:1211.0379 [gr-qc]].
- [45] T. Kitamura, *Astrometric microlensing by the Ellis Wormhole*
- [46] Y. Toki, T. Kitamura, H. Asada and F. Abe, *Astrophys. J.* **740** (2011), 121 doi:10.1088/0004-637X/740/2/121 [arXiv:1107.5374 [astro-ph.CO]].
- [47] F. Abe, *Astrophys. J.* **725** (2010), 787–793 doi:10.1088/0004-637X/725/1/787 [arXiv:1009.6084 [astro-ph.CO]].
- [48] M. B. Bogdanov and A. M. Cherepashchuk, *Astrophys. Space Sci.* **317** (2008), 181–192 doi:10.1007/s10509-008-9870-z [arXiv:0807.2774 [astro-ph]].
- [49] D. F. Torres, E. F. Eiroa and G. E. Romero, *Mod. Phys. Lett. A* **16** (2001), 1849–1861 doi:10.1142/S0217732301005126 [arXiv:gr-qc/0109041 [gr-qc]].

- [50] M. Safonova, D. F. Torres and G. E. Romero, *Phys. Rev. D* **65** (2002), 023001 doi:10.1103/PhysRevD.65.023001 [arXiv:gr-qc/0105070 [gr-qc]].
- [51] D. F. Torres, G. E. Romero and L. A. Anchordoqui, *Mod. Phys. Lett. A* **13** (1998), 1575-1582 doi:10.1142/S0217732398001650 [arXiv:gr-qc/9805075 [gr-qc]].
- [52] D. F. Torres, G. E. Romero and L. A. Anchordoqui, *Phys. Rev. D* **58** (1998), 123001 doi:10.1103/PhysRevD.58.123001 [arXiv:astro-ph/9802106 [astro-ph]].
- [53] G. W. Gibbons and M. C. Werner, *Class. Quant. Grav.* **25** (2008), 235009 doi:10.1088/0264-9381/25/23/235009 [arXiv:0807.0854 [gr-qc]].
- [54] G. W. Gibbons, C. A. R. Herdeiro, C. M. Warnick and M. C. Werner, *Phys. Rev. D* **79** (2009), 044022 doi:10.1103/PhysRevD.79.044022 [arXiv:0811.2877 [gr-qc]].
- [55] M. C. Werner, *Gen. Rel. Grav.* **44** (2012), 3047-3057 doi:10.1007/s10714-012-1458-9 [arXiv:1205.3876 [gr-qc]].
- [56] X. He, T. Xu, Y. Yu, A. Karamat, R. Babar and R. Ali, *Annals Phys.* **451** (2023), 169247 doi:10.1016/j.aop.2023.169247
- [57] S. Upadhyay, S. Mandal, Y. Myrzakulov and K. Myrzakulov, *Annals Phys.* **450** (2023), 169242 doi:10.1016/j.aop.2023.169242 [arXiv:2303.02132 [gr-qc]].
- [58] W. Javed, M. Atique, R. C. Pantig and A. Övgün, *Symmetry* **15** (2023) no.1, 148 doi:10.3390/sym15010148 [arXiv:2301.01855 [gr-qc]].
- [59] W. Javed, H. Irshad, R. C. Pantig and A. Övgün, *Universe* **8** (2022) no.11, 599 doi:10.3390/universe8110599 [arXiv:2211.07009 [gr-qc]].
- [60] Y. Huang and Z. Cao, *Phys. Rev. D* **106** (2022) no.10, 104043 doi:10.1103/PhysRevD.106.104043
- [61] J. He, Q. Wang, Q. Hu, L. Feng and J. Jia, *Class. Quant. Grav.* **40** (2023) no.6, 065006 doi:10.1088/1361-6382/acbade [arXiv:2210.00938 [gr-qc]].
- [62] X. J. Gao, X. k. Yan, Y. Yin and Y. P. Hu, [arXiv:2303.00190 [gr-qc]].
- [63] T. Cai, Z. Wang, H. Huang and M. Zhu, [arXiv:2302.13704 [gr-qc]].
- [64] A. Övgün, R. C. Pantig and Á. Rincón, *Eur. Phys. J. Plus* **138** (2023) no.3, 192 doi:10.1140/epjp/s13360-023-03793-w [arXiv:2303.01696 [gr-qc]].
- [65] F. S. N. Lobo, *Phys. Rev. D* **71** (2005), 084011 doi:10.1103/PhysRevD.71.084011 [arXiv:gr-qc/0502099 [gr-qc]].
- [66] F. S. N. Lobo, *Phys. Rev. D* **71** (2005), 124022 doi:10.1103/PhysRevD.71.124022 [arXiv:gr-qc/0506001 [gr-qc]].
- [67] R. Garattini and F. S. N. Lobo, *Class. Quant. Grav.* **24** (2007), 2401-2413 doi:10.1088/0264-9381/24/9/016 [arXiv:gr-qc/0701020 [gr-qc]].
- [68] K. Nakajima and H. Asada, *Phys. Rev. D* **85** (2012), 107501 doi:10.1103/PhysRevD.85.107501 [arXiv:1204.3710 [gr-qc]].
- [69] K. Jusufi, *Int. J. Geom. Meth. Mod. Phys.* **14** (2017) no.12, 1750179 doi:10.1142/S0219887817501791 [arXiv:1706.01244 [gr-qc]].
- [70] S. W. Kim and H. Lee, *Phys. Rev. D* **63**, 064014 (2001) doi:10.1103/PhysRevD.63.064014 [arXiv:gr-qc/0102077 [gr-qc]].
- [71] K. Jusufi, A. Övgün, A. Banerjee and . I. Sakalli, *Eur. Phys. J. Plus* **134** (2019) no.9, 428 doi:10.1140/epjp/i2019-12792-9 [arXiv:1802.07680 [gr-qc]].
- [72] M. D. Johnson, A. Lupsasca, A. Strominger, G. N. Wong, S. Hadar, D. Kapec, R. Narayan, A. Chael, C. F. Gammie and P. Galison, *et al. Sci. Adv.* **6** (2020) no.12, eaaz1310 doi:10.1126/sciadv.aaz1310 [arXiv:1907.04329 [astro-ph.IM]].
- [73] S. E. Gralla and A. Lupsasca, *Phys. Rev. D* **101** (2020) no.4, 044031 doi:10.1103/PhysRevD.101.044031 [arXiv:1910.12873 [gr-qc]].
- [74] M. Alcubierre and F. S. N. Lobo, "Wormholes, Warp Drives and Energy Conditions," *Fundam. Theor. Phys.* **189** (2017), pp.-279 Springer, 2017, doi:10.1007/978-3-319-55182-1 [arXiv:2103.05610 [gr-qc]].
- [75] J. Zaris, D. Veske, J. Samsing, Z. Márka, I. Bartos and S. Márka, *Astrophys. J. Lett.* **894** (2020) no.1, L9 doi:10.3847/2041-8213/ab89a3 [arXiv:1912.05701 [astro-ph.HE]].
- [76] A. Sollima, M. Bellazzini, R. L. Smart, M. Correnti, E. Pancino, F. R. Ferraro and D. Romano, *Mon. Not. Roy. Astron. Soc.* **396** (2009), 2183 doi:10.1111/j.1365-2966.2009.14864.x [arXiv:0904.0571 [astro-ph.SR]].
- [77] E. Noyola, K. Gebhardt, M. Kissler-Patig, N. Lutzgendorf, B. Jalali, P. T. de Zeeuw and H. Baumgardt, *Astrophys. J. Lett.* **719** (2010), L60 doi:10.1088/2041-8205/719/1/L60 [arXiv:1007.4559 [astro-ph.GA]].
- [78] F. Kiroğlu, N. C. Weatherford, K. Kremer, C. S. Ye, G. Fragione and F. A. Rasio, *Astrophys. J.* **928** (2022) no.2, 181 doi:10.3847/1538-4357/ac5895 [arXiv:2111.14866 [astro-ph.GA]].
- [79] R. G. Cai, T. Chen, S. J. Wang and X. Y. Yang, *JCAP* **03** (2023), 043 doi:10.1088/1475-7516/2023/03/043 [arXiv:2210.02078 [astro-ph.CO]].